


Geometric Sampling

Bardia Panahbehagh

panahbehagh@khu.ac.ir ,

*Faculty of Mathematical Sciences and Computer, Kharazmi University,
Tehran, Iran*

Abstract: This paper introduces an innovative and intuitive finite population sampling method that have been developed using a unique geometric framework. In this approach, I represent first-order inclusion probabilities as bars on a two-dimensional graph. By manipulating the positions of these bars, researchers can create a wide range of different sampling designs. This geometric visualization of sampling designs not only leads to increased creativity for researchers to provide new efficient designs but also eliminates the need for complex mathematical algorithms. This novel approach holds significant promise for tackling complex challenges in sampling, such as maximizing entropy and achieving an optimal design. By applying a version of the greedy best-first search algorithm to this geometric approach for finding an optimal design, I have demonstrated the potential for integrating intelligent algorithms into finite population sampling.

MSC2020 subject classifications: Primary 62D05, 62F40; secondary 94A17.

Keywords and phrases: Inclusion Probabilities, Maximum Entropy Design, Sampling Design, Intelligent Algorithm.

1. Introduction

The conventional approach to finite population sampling is to deal with sets and indices that can be seen in reference book such as Tillé (2020) as follows. Let $U = \{1, \dots, N\}$ be a population of size N , and define

$$\mathcal{S} = \{s_1, s_2, \dots, s_T\}.$$

as the set of all the possible samples or subsets. The aim is to select a sample S of \mathcal{S} with first-order inclusion probabilities (FIP) $\boldsymbol{\pi} = \{\pi_k, k \in U\}$, and size n_s where

$$\sum_{k \in U} \pi_k = E(n_s).$$

Let $\mathbf{p} = \{p_t = Pr(S = s_t); t = 1, 2, \dots, T\}$ be a sampling design that assigns a probability to each possible sample such that

$$\sum_{t=1}^T p_t = 1, \text{ and } \sum_{t: s_t \ni k} p_t = \pi_k \text{ for all } k \in U. \quad (1)$$

The second-order inclusion probabilities (SIP) can be represented in matrix form as follows

$$\Pi = [\pi_{k\ell}]_{N \times N}, \text{ where } \pi_{k\ell} = \sum_{t: s_t \ni k, \ell} p_t, \quad k, \ell \in U.$$

Also entropy of design \mathbf{p} is defined as

$$H(\mathbf{p}) = - \sum_{t=1}^T p_t \ln(p_t).$$

Now consider $y_k, x_k, k \in U$ as the main and auxiliary variables respectively. The main goal of sampling is typically to estimate parameters such as the population total, denoted by,

$$Y = \sum_{k \in U} y_k.$$

The estimation of parameters involving total estimation and its variance is based on the designs, FIP, and SIP. We can estimate Y unbiasedly by the Narain-Horvitz-Thompson (Narain, 1951; Horvitz and Thompson, 1952) estimator (NHT),

$$\hat{Y} = \sum_{k \in S} \frac{y_k}{\pi_k},$$

with

$$var(\hat{Y}) = \sum_{k \in U} \sum_{\ell \in U} \frac{y_k}{\pi_k} \frac{y_\ell}{\pi_\ell} (\pi_{k\ell} - \pi_k \pi_\ell), \quad (2)$$

and given all the $\pi_{k\ell}$ are positive, an unbiased estimator

$$v\hat{ar}(\hat{Y}) = \sum_{k \in S} \sum_{\ell \in S} \frac{y_k}{\pi_k} \frac{y_\ell}{\pi_\ell} \frac{\pi_{k\ell} - \pi_k \pi_\ell}{\pi_{k\ell}}, \quad (3)$$

or for fixed-size designs, defined as $Var(n_s) = 0$ in designs with integer $E(n_s)$, a more stable estimator as

$$v\hat{ar}(\hat{Y}) = \frac{1}{2} \sum_{k \in S} \sum_{\ell \in S} \left(\frac{y_k}{\pi_k} - \frac{y_\ell}{\pi_\ell} \right)^2 \frac{\pi_{k\ell} - \pi_k \pi_\ell}{\pi_{k\ell}}. \quad (4)$$

This conventional approach employs designs rooted in theoretical and mathematical algorithms, which can obscure comprehension and prove challenging to implement. In finite population sampling, improving the efficiency of sampling designs often leads to increased complexity in

calculating probabilities, such as FIP and SIP, which are essential for accurate estimation and assessment. As an example consider probability proportional to size sampling (PPS). In this unequal probability design, the sample units are selected proportional to size of an auxiliary variable which will be an efficient design if the auxiliary variable be correlated to the main variable. Design with unequal probabilities with replacement is first introduced by ansen and Hurwitz (1943). Madow (1949), Narain (1951), and Horvitz and Thompson (1952) proposed without replacement versions of PPS. Selecting a PPS sample, without replacement and with a fixed sample size, is a complex procedure. For this purpose, many different designs have been proposed whose 50 of which are listed in Brewer and Hanif (1983) and Tillé (2006, 2020). All these 50 designs can implement PPS that satisfy FIP (leading unbiasedly estimating certain parameters using the NHT estimator), but may lead to different SIP, affecting estimation precision. While implementing an unequal probability, without replacement, fixed-size design has been solved, finding a design within this space, with higher precision remains an open problem and then investigating which combinations of SIP yield an optimal PPS is intriguing.

The core concept of this new approach is an unequal probability, without replacement and fixed-size sampling method. A simplified version of the approach aligns with Madow (1949), inheriting its limitation of many zero SIP. However, the proposed approach offers significant flexibility which, when combined with the preservation of FIP, allows the method to encompass all existing unequal probability sampling designs and explore new possibilities. By modifying the SIP matrix in various ways, it can mimic other designs like simple random sampling, stratified sampling, multi-stage sampling, Poisson sampling, and maximum entropy sampling (Tillé 2006), etc. Unifying diverse designs within a single framework opens doors to explore optimal sampling designs. For this exploration, GFS can serve as a bridge between the theoretical concepts of finite population sampling and the practical implementation of computer algorithms, providing a novel approach to designing efficient and effective sampling designs.

In Section 2, I present the new approach. Section 3 discusses reducing zero SIP, leading to Poisson sampling. In Section 4, I show that a simple fixed-size version of the method is equivalent to Madow (1949) and reducing zero SIP in the this version leads to maximum entropy sampling. Section 5 introduces an intelligent methods for searching optimal design. In Section 6 some simulations are conducted. Finally, Section 7 concludes the article with a summary and suggestions.

2. A Geometric Approach to Finite Population Sampling (GFS)

For sampling with a predetermined FIP, $\boldsymbol{\pi}$, I propose a geometric approach presented in Algorithm 1;

Algorithm 1 GFS

- 1: Create a two-dimensional coordinate system, indicate the population units on the horizontal axes, and consider the vertical axis for the FIP between 0 and 1,
 - 2: **for** $k = 1, 2, \dots, N$ **do**
 - 3: Draw a bar of length π_k above point k at an arbitrary or random position such that the bar is completely between 0 and 1,
 - 4: **end for**
 - 5: Select a random point, say r between 0 and 1, plot it on the vertical axes, and draw a horizontal line, say a random line, from the selected point,
 - 6: The final sample units are all units for which the random line passes through the bars of their FIP.
-

Figure 1 provides an example of Algorithm 1 with

$$\boldsymbol{\pi} = \{.38, .30, .42, .65, .25, .10, .90\}, \quad (5)$$

each in different color. The two top plots in Figure 1 illustrate two different arrangements of bars, each representing a distinct design. Both arrangements adhere to the FIP constraint. The accompanying designs (samples and probabilities) on the left, illustrate that any modification in the bar positions results in a new design, as shown by transitioning from design \boldsymbol{p} with $T = 9$ in the top plot to design \boldsymbol{p}^* with $T = 10$ in the middle plot, where the bars for π_4 , π_5 , π_6 , and π_7 have been rearranged. The bottom plot in Figure 1 presents two examples in design \boldsymbol{p}^* to illustrate different concepts related to GFS:

- The first example demonstrates how to calculate the SIP of units, which can be determined by finding the intersection of the bars. In this illustration, the SIP for units $k = 2$ and $\ell = 3$ is highlighted in gray, resulting in a value of $\pi_{k\ell} = .12$ as specified by the design.
- The second example involves drawing random line, shown as a black line, $r = .15$. This random line passes through the FIP of units 1, 5 and 7, thereby selecting these three units as the final sample. This visual demonstrates how a random selection process can determine the final sample based on GFS.

Then using GFS, by preserving FIP, we can estimate Y unbiasedly, and by rearranging the bars, we can change SIP and then control the variance, or in other words, the precision of the estimation.

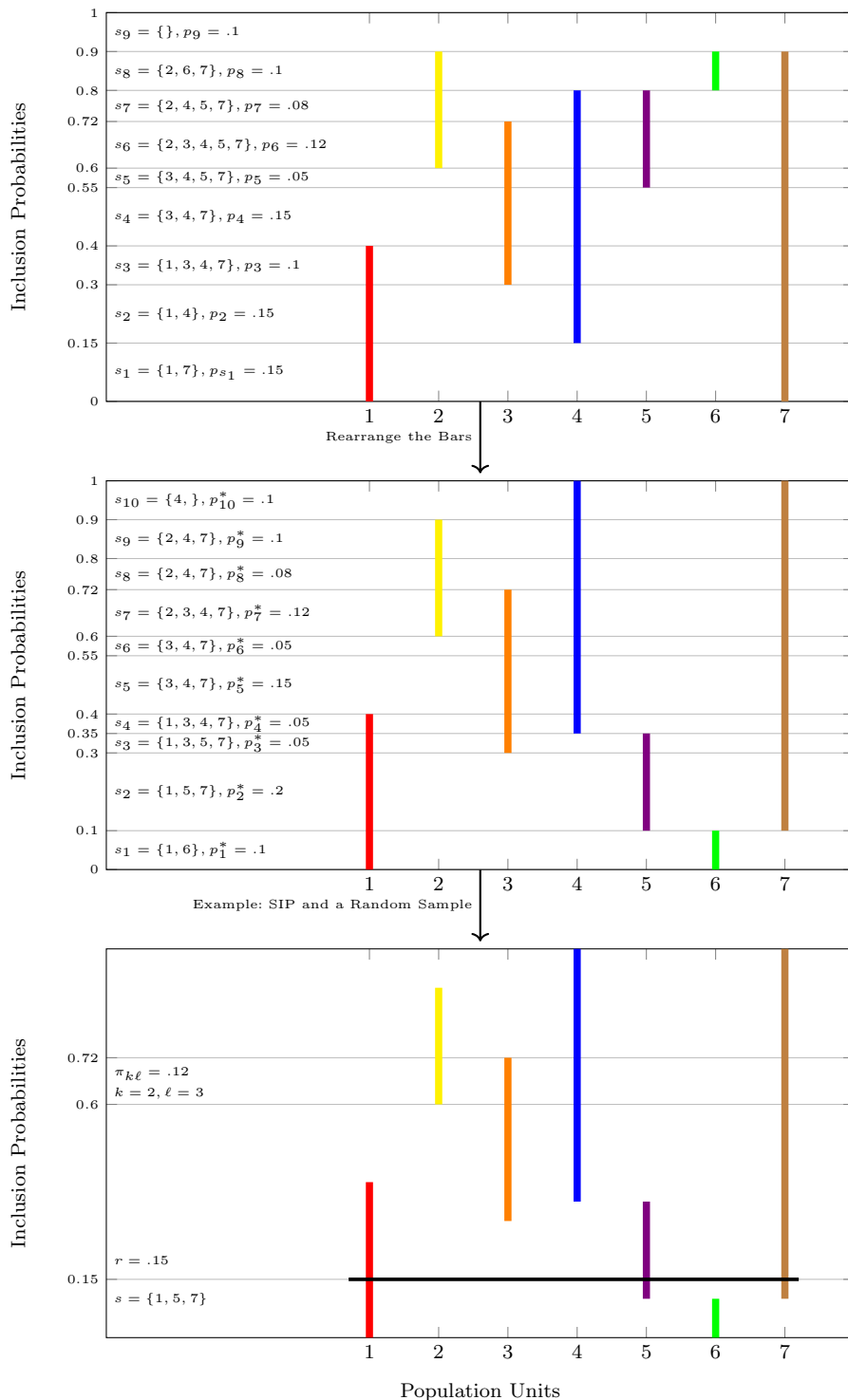


FIG 1. The two top plots depict different arbitrary arrangements of bars with $\pi = \{.38, .30, .42, .65, .25, .10, .90\}$ in different colors based on Algorithm 1, in which both arrangements respect FIP. The designs (\mathbf{p} and \mathbf{p}^*) are calculated and presented on the left of the plots, showing that any change in the position of the bars results in creating a new design. The bottom plot illustrates two examples: (1) The calculation of the SIP for units $k = 2$ and $\ell = 3$, highlighted in gray, resulting in $\pi_{k\ell} = .12$, (2) A random line (horizontal black line) is drawn, selecting units 1, 5 and 7 as the final sample, $s = \{1, 5, 7\}$.

It is notable that in GFS, after selecting the final sample, since we have all the SIP, we can easily estimate the variance of the NHT estimator using Equation (3). The next Result indicates that the method preserves the FIP.

Theorem 2.1. *In the GFS approach, with any arrangement of the bars,*

$$Pr(k \in S) = \pi_k; \quad k = 1, 2, \dots, N, \quad E(n_s) = \sum_{k \in U} \pi_k.$$

Proof. The proof follows directly from Algorithm 1. □

Algorithm 1 suffers from two key limitations: a high propensity for zero SIP and variable sample size. As an example consider top plot in Figure 1, where the sample size fluctuates among $n_s = 0, 2, 3, 4, 5$, and the SIP for $k = 1, \ell = 2, 5, 6$ are all zero. These deficiencies warrant further exploration, as they significantly impact the algorithm's efficiency and applicability in real-world scenarios. Subsequent sections present novel algorithms specifically developed to overcome these limitations, significantly improving the overall effectiveness of the sampling process.

3. Increasing Design Entropy: A Strategy for Decreasing Zero SIP

Even a zero element in the SIP matrix results in no unbiased estimators for variance of the NHT estimator. Then it will be interesting to introduce a design with a positive SIP matrix. In this section, I propose an algorithm for the reduction of the zero elements in the SIP matrix.

To begin, consider the y -axis partitioned into D strips, denoted by $\Delta_1, \Delta_2, \dots, \Delta_D$, corresponding to the samples s_1, s_2, \dots, s_D . Note that $D \geq T$, as some samples may appear multiple times across the y -axis partitioning. Now, select two strips, Δ_i and Δ_j , with respective heights p_i and p_j . Inside each strip, consider two smaller substrips δ_i and δ_j , both of size $v_{i,j}(\alpha) = \alpha \times \min(p_i, p_j)$ for $\alpha \in [0, 1]$, and define:

$$\delta_i(k) = \begin{cases} 1 & \text{if the bar on unit } k \text{ completely covers the height of substrip } \delta_i, \\ 0 & \text{otherwise.} \end{cases}$$

Next, if $s_{i-j} = s_i \setminus s_j$ is nonempty, select $k \in s_{i-j}$ and interchange the segment of π_k in δ_i with δ_j . In other words, set $\delta_i(k) = 0$ and $\delta_j(k) = 1$, which potentially leads to the following outcomes:

- sample s_i with probability p_i splitting into two samples:

$$1: s_{i,1} = s_i, \quad p_{i,1} = p_i - v_{i,j}(\alpha),$$

$$2: s_{i,2} = s_i \setminus \{k\}, \quad p_{i,2} = v_{i,j}(\alpha),$$

- sample s_j with probability p_j splitting into two samples:

$$3: s_{j,1} = s_j, \quad p_{j,1} = p_j - v_{i,j}(\alpha),$$

$$4: s_{j,2} = s_j \cup \{k\}, \quad p_{j,2} = v_{i,j}(\alpha).$$

In summary, to reduce zero SIP, in Algorithm 1, we can select a piece of a bar and change its position provided there is an empty space in the new position. Details are given in Algorithm 2.

Algorithm 2 Poisson Sampling, Chaotic GFS

- 1: Create a two-dimensional coordinate system, placing the population units on the horizontal axis and using the vertical axis for FIP, ranging from 0 to 1, and built the sampling design,
 - 2: **for** $m = 1, 2, \dots, M$ **do**
 - 3: Select randomly two strips Δ_i and Δ_j , and within them two substrips δ_i and δ_j of size $v_{i,j}(\alpha)$ with $0 < \alpha < 1$,
 - 4: **if** s_{i-j} is not empty **then**
 - 5: select $k \in s_{i-j}$ randomly,
 - 6: set $\delta_i(k) = 0$ and $\delta_j(k) = 1$,
 - 7: **end if**
 - 8: **end for**
 - 9: Draw a random line,
 - 10: The final sample consists of all units for which the random line passes through their respective bars of FIP.
-

To elucidate the core concept of Algorithm 2, examine the plots in Figure 2. In the top plot, consider Δ_2 and Δ_5 and within them observe that $\delta_5(4) = 1$ and $\delta_2(4) = 0$. Subsequently, we can truncate the corresponding segment of π_4 in δ_5 and relocate it to the new position in δ_2 , resulting in $\delta_2(4) = 1$ and $\delta_5(4) = 0$, as depicted in the bottom plot. This implementation of Algorithm 2 with $M = 1$ increases the entropy of the design or in other words leads to more possible samples. For example, in the top plot, $\pi_{k\ell} = 0$ for $k = 4$ and $\ell = 5$, while after increasing the entropy, we have $\pi_{k\ell} = 0.07$ for $k = 4$ and $\ell = 5$.

It is noteworthy that SIP is fully computable in GFS. Even if we increase the design's entropy by exchanging segments using a random procedure, the SIP ultimately reverts to the most recent fixed design, as our sampling is eventually performed based on a stabilized configuration.

Crucially, the following result demonstrates that, under Chaotic GFS, the probability of obtaining any design other than Poisson sampling becomes vanishingly small.

Theorem 3.1. *Chaotic GFS converges to Poisson sampling as $M \rightarrow \infty$.*

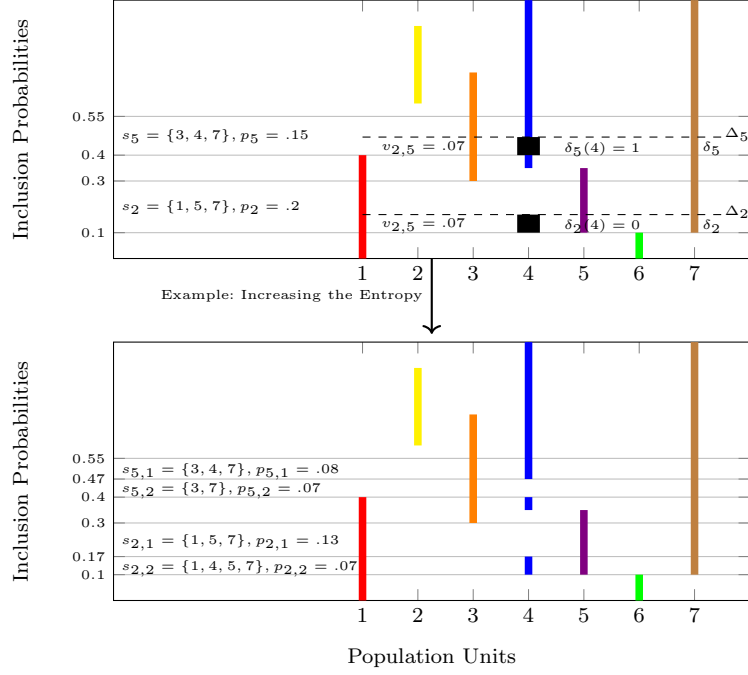


FIG 2. An example of entropy enhancement in the design \mathbf{p}^* (the middle plot of Figure 1). By selecting Δ_2 and Δ_5 with sizes $p_2^* = 0.2$ and $p_5^* = 0.15$, and choosing substrips δ_2 and δ_5 of size $v_{2,5}(7/15) = 0.07$, it is possible to interchange segments between substrips δ_2 and δ_5 for unit $k = 4$, which leads to four samples: $s_{2,1}$, $s_{2,2}$, $s_{5,1}$, and $s_{5,2}$.

Proof. The proof is inspired by the work of Jaynes (1957). Here, I initially prove that the probability of each design being formed by Chaotic GFS is proportional to the design entropy. Then, I demonstrate that any design is exponentially less likely than Poisson sampling to be achieved by Chaotic GFS. For this purpose, first I prove that

$$Pr(\mathbf{P} = \mathbf{p}|\boldsymbol{\pi}) \simeq \frac{e^{DH(\mathbf{p})}}{B},$$

where D is the number of strips, B is some normalized constant, $Pr(\mathbf{P} = \mathbf{p}|\boldsymbol{\pi})$ is the probability of reaching design \mathbf{p} in the chaotic GFS process. Indeed, D is a function of M , however, for simplicity of notation, we omitted it.

Consider \mathbf{P} as a design defined on the power set of U , with $T = 2^N$. Following Algorithm 2, it is easy to prove that for sufficiently large M , the y-axis in $[0, 1]$ will be partitioned into D strips (almost at the same size), in which $D_t, t = 1, 2, \dots, T$ of them corresponds to s_t .

Therefore

$$Pr(\mathbf{P} = \mathbf{p}|\boldsymbol{\pi}) = \lim_{M \rightarrow \infty} \frac{\binom{D}{D_1, D_2, \dots, D_T}}{\prod_{k=1}^N \binom{D}{D(k)}},$$

where $D_t = Dp_t$ is the number of strips of size $1/D$ on the vertical axis for s_t and $D(k) = D\pi_k$ is number of strips occupied by π_k on the unit k . Now using Stirling approximation we have

$$\begin{aligned} \binom{D}{D_1, D_2, \dots, D_T} &= \frac{D!}{\prod_{t=1}^T Dp_t!} \simeq \frac{(2\pi D)^{-\frac{T-1}{2}} D^D e^{-D}}{\prod_{t=1}^T p_t^{.5} D^{Dp_t} p_t^{Dp_t} e^{-Dp_t}} = \frac{(2\pi D)^{-\frac{T-1}{2}}}{\prod_{t=1}^T p_t^{.5} p_t^{Dp_t}} \\ &= e^{-\frac{T-1}{2} \ln(2\pi D) - D \sum_{t=1}^T p_t \ln(p_t) - .5 \sum_{t=1}^T \ln p_t}. \end{aligned}$$

Also for denominator, we set

$$1 / \prod_{k=1}^N \binom{D}{D(k)} = g(\boldsymbol{\pi}, D),$$

as a constant function of \mathbf{p} . Therefore

$$\begin{aligned} Pr(\mathbf{P} = \mathbf{p} | \boldsymbol{\pi}) &\simeq g(\boldsymbol{\pi}, D) e^{-\frac{(T-1)}{2} \ln(2\pi D) - \frac{1}{2} \sum_{t=1}^T \ln(Dp_t) - D \sum_{t=1}^T p_t \ln(p_t)} \\ &= g(\boldsymbol{\pi}, D) e^{-D \sum_{t=1}^T p_t \ln(p_t) (1 + O(\frac{1}{D}))} \\ &= g(\boldsymbol{\pi}, D) e^{DH(\mathbf{p}) (1 + O(\frac{1}{D}))}. \end{aligned} \quad (6)$$

For sufficiently large M (or equivalently, large D), the term involving $DH(\mathbf{p})$ dominates the other terms. Then, given that $g(D, \boldsymbol{\pi})$ is a constant, we have

$$Pr(\mathbf{P} = \mathbf{p} | \boldsymbol{\pi}) \propto e^{DH(\mathbf{p})} = \frac{e^{DH(\mathbf{p})}}{B},$$

for some constant B .

Now I show that, any design is exponentially less likely than Poisson sampling, to be obtained in Chaotic GFS. Consider a sampling design based on $\boldsymbol{\pi}$, say \mathbf{q} with $H(\mathbf{q})$, and also consider Poisson sampling, say \mathbf{p} . As \mathbf{p} has the maximum entropy given $\boldsymbol{\pi}$, we have

$$H(\mathbf{q}) = H(\mathbf{p}) - \varepsilon, \quad \varepsilon > 0.$$

Then,

$$Pr(\mathbf{P} = \mathbf{q} | \boldsymbol{\pi}) = \lim_{D \rightarrow \infty} \frac{e^{DH(\mathbf{q})}}{B} = \lim_{D \rightarrow \infty} \frac{e^{DH(\mathbf{p})}}{B} e^{-D\varepsilon}.$$

Therefore as

$$e^{DH(\mathbf{p})}/B < \infty, \quad \text{and} \quad \lim_{D \rightarrow \infty} e^{-D\varepsilon} = 0,$$

for large enough D , we have

$$Pr(\mathbf{P} = \mathbf{q} | \boldsymbol{\pi}) = 0.$$

□

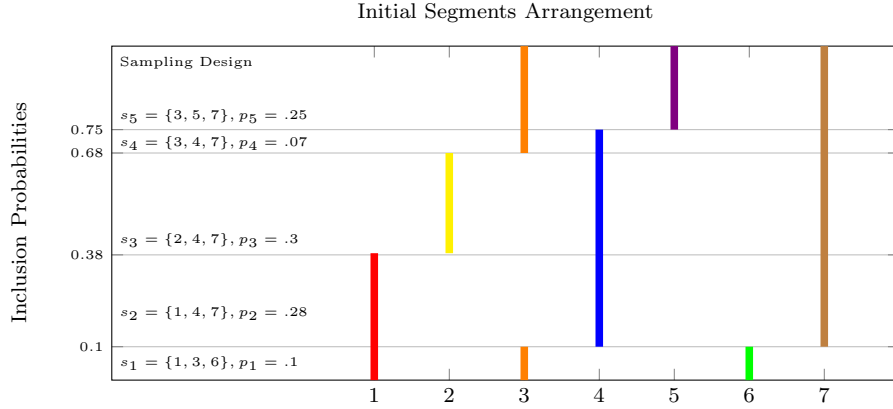


FIG 3. The plot depicts a fixed-size version (Algorithm 3) of GFS with $\pi = \{.38, .3, .42, .65, .25, .1, .9\}$, arranged sequentially to create a fixed-size design.

4. Fixed-size Algorithm of GFS

Building upon the resolution of the entropy issue in the previous section, the subsequent section focuses on tackling the challenge of random sample size within the framework of Algorithm 1.

To overcome this challenge, one of the simplest approaches is to arrange the bars based on a cumulative manner as follows. The first bar starts from zero to π_1 , the second bar starts from π_1 to $\min(\pi_1 + \pi_2, 1)$, and if the minimum is 1, then the remainder of $(\pi_1 + \pi_2) - 1$ continues from zero, and so forth. Details are presented in Algorithm 3.

Algorithm 3 Fixed-size GFS, equivalent to Madow (1949)

- 1: In Algorithm 1, the first bar covers $[0, \pi_1]$, and set $b_1 = \pi_1$,
 - 2: **for** $k = 2, 3, \dots, N$ **do**
 - 3: **if** $\pi_k + b_{k-1} \leq 1$ **then** k^{th} bar covers $(b_{k-1}, \pi_k + b_{k-1}]$, set $b_k = \pi_k + b_{k-1}$,
 - 4: **else** k^{th} bar covers $(b_{k-1}, 1] \cup [0, \pi_k + b_{k-1} - 1]$, set $b_k = \pi_k + b_{k-1} - 1$,
 - 5: **end if**
 - 6: **end for**
-

Figure 3 presents a fixed-size version of GFS with $\pi = \{.38, .3, .42, .65, .25, .1, .9\}$ arranged sequentially to form a design with fixed size $n = \sum_{k=1}^7 \pi_k = 3$. In this arrangement, the FIP are aligned in a way that maintains the fixed size constraint.

Interestingly, Algorithm 3 can be viewed as a vertical adaptation of the systematic sampling method proposed by Madow (1949). However, in the following, I will demonstrate that unlike systematic sampling described by Madow (1949), this novel approach possesses the capability to emulate various traditional and novel designs, including many fixed-size unequal probability

sampling methods.

To increase the entropy of the Madow version of GFS, a strategy similar to the one described in Section 3 can be applied. Specifically, two strips of two samples can be selected, and two segments of their bars can be interchanged, provided that an empty space exists in the new positions. This approach preserves fixed sample sizes while increasing entropy. However, to present a complete algorithm for this process, it is necessary to define two key concepts.

First, define:

Definition 4.1. Consider two substrips on the vertical axis, $\delta_i \subseteq \Delta_i$ and $\delta_j \subseteq \Delta_j$. Two segments, $\delta_i(k)$ and $\delta_j(\ell)$, are interchangeable if

$$\delta_i(k) = 1, \quad \delta_j(\ell) = 1; \quad \delta_j(k) = 0, \quad \delta_i(\ell) = 0.$$

Definition 4.2. Interchanging two interchangeable segments $\delta_i(k)$ and $\delta_j(\ell)$ means setting

$$\delta_i(k) = 0, \quad \delta_j(\ell) = 0; \quad \delta_j(k) = 1, \quad \delta_i(\ell) = 1.$$

Now, consider two strips Δ_i and Δ_j with heights p_i and p_j , and two substrips δ_i and δ_j of the same size $v_{ij}(\alpha)$. If s_{i-j} and s_{j-i} are nonempty, select $k \in s_{i-j}$ and $\ell \in s_{j-i}$ randomly, and interchange them, potentially leading to:

- Sample s_i with probability p_i splits into two samples:

$$1: s_{i,1} = s_i, \quad p_{i,1} = p_i - v_{i,j}(\alpha),$$

$$2: s_{i,2} = s_i \cup \{\ell\} \setminus \{k\}, \quad p_{i,2} = v_{i,j}(\alpha),$$

- Sample s_j with probability p_j splits into two samples:

$$3: s_{j,1} = s_j, \quad p_{j,1} = p_j - v_{i,j}(\alpha),$$

$$4: s_{j,2} = s_j \cup \{k\} \setminus \{\ell\}, \quad p_{j,2} = v_{i,j}(\alpha).$$

Details are presented in Algorithm 4.

Algorithm 4 Chaotic fixed-size GFS

- 1: Implement Algorithm 3.
 - 2: **for** $m = 1, 2, \dots, M$ **do**
 - 3: Select randomly two strips Δ_i and Δ_j , and within them two substrips δ_i and δ_j with size $\delta_{i,j}(\alpha)$, $0 < \alpha < 1$,
 - 4: **if** s_{i-j} and s_{j-i} are not empty **then**,
 - 5: select $k \in s_{i-j}$ and $\ell \in s_{j-i}$ randomly,
 - 6: Interchange $\delta_i(k)$ and $\delta_j(\ell)$.
 - 7: **end if**
 - 8: **end for**
-

As an example of Algorithm 4, consider Figure 4, in which two strips, Δ_2 and Δ_5 , are selected and by using two substrips of size $v_{2,5}(10/25) = .1$, segments of units 1 and 5 are interchanged to increase the entropy of the design.

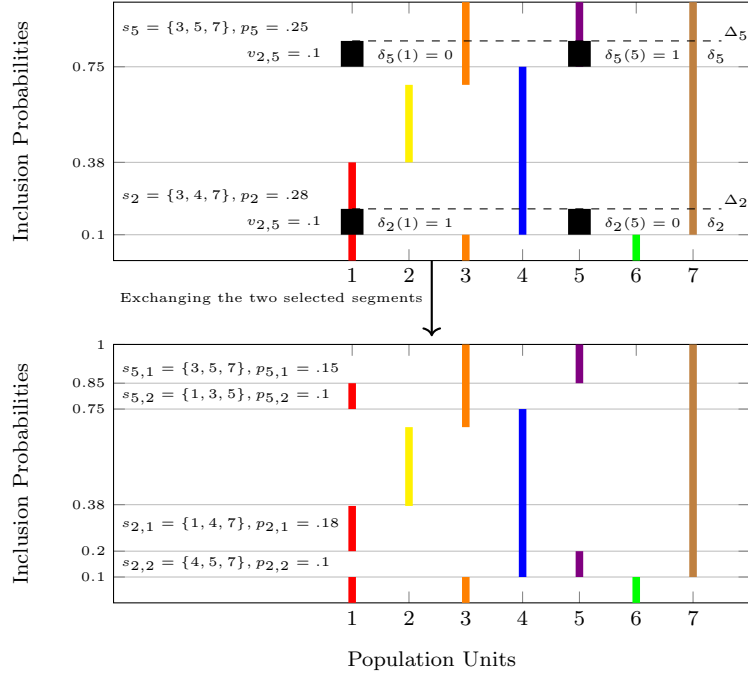


FIG 4. The top plot depicts a fixed-size version of GFS with $\pi = \{0.38, 0.30, 0.42, 0.65, 0.25, 0.10, 0.90\}$, arranged sequentially to create a fixed-size design in which two strips, Δ_2 and Δ_5 , are selected. Within these strips, two substrips of size $v_{2,5} = 0.10$ are indicated by dashed lines. Since units 1 and 5 are interchangeable in this situation, they are interchanged, resulting in two new samples, $s_{2,2}$ and $s_{5,2}$, alongside the original samples, $s_{2,1}$ and $s_{5,1}$, depicted in the bottom plot.

As an interesting result, implementing the Chaotic fixed-size GFS results in fixed-size Poisson sampling, also known as conditional Poisson sampling or maximum entropy sampling.

Theorem 4.3. In the Chaotic fixed-size GFS approach, based on Algorithms 4,

$$Pr(k \in S) = \pi_k; \quad k = 1, 2, \dots, N,$$

$$E(n_s) = \sum_{k \in U} \pi_k,$$

and if $E(n_s)$ is an integer, the design will be Fixed-size or in other words:

$$var(n_s) = .$$

Proof. The proof follows directly from Algorithms 4. □

Theorem 4.4. *Chaotic fixed-size GFS with $M \rightarrow \infty$, convergences to maximum entropy sampling.*

Proof. Consider the following condition

$$\mathbb{C} = \left\{ \mathbf{p}; \sum_{t=1}^T [n_t - E(n_t)]^2 p_t = 0; \sum_{t; s_t \ni k} p_t = \pi_k \right\}$$

where n_t is the size of s_t . Then,

$$Pr(\mathbf{P} = \mathbf{p} | \mathbb{C}) = \begin{cases} \lim_{M \rightarrow \infty} \frac{\binom{D}{D_1, D_2, \dots, D_T}}{B_c}, & \mathbf{p} \in \mathbb{C} \\ 0, & \text{o.w.} \end{cases} \quad (7)$$

where B_c is a normalized constant based on \mathbb{C} as

$$B_c = \sum_{\mathbf{p} \in \mathbb{C}} \binom{D}{Dp_1, Dp_2, \dots, Dp_T}.$$

Then similar to Equation (6) we have

$$Pr(\mathbf{P} = \mathbf{p} | \mathbb{C}) \propto e^{D\mathbb{H}(\mathbf{p})(1+O(\frac{1}{D}))},$$

where $\mathbb{H}(\mathbf{p}) = H(\mathbf{p} | \mathbb{C})$. Therefore, for large enough D , we have $Pr(\mathbf{P} = \mathbf{p} | \mathbb{C}) \propto e^{D\mathbb{H}(\mathbf{p})}$.

Also based on the same approach in proof of Theorem 3.1, again consider \mathbf{p} as the design with the maximum entropy under \mathbb{C} and \mathbf{q} as any other design in \mathbb{C} with $\mathbb{H}(\mathbf{p}) = \mathbb{H}(\mathbf{q}) + \varepsilon$ for an $\varepsilon > 0$. We have

$$Pr(\mathbf{P} = \mathbf{q} | \mathbb{C}) \propto e^{D\mathbb{H}(\mathbf{q})} = e^{D\mathbb{H}(\mathbf{p})} e^{-D\varepsilon} = 0,$$

which will be exponentially less likely than the maximum entropy design. \square

Figure 5 illustrates a maximum entropy sampling design of the data in population (5) utilizing Algorithm 4 with $\alpha = 0.5$ and $M = 10,000$.

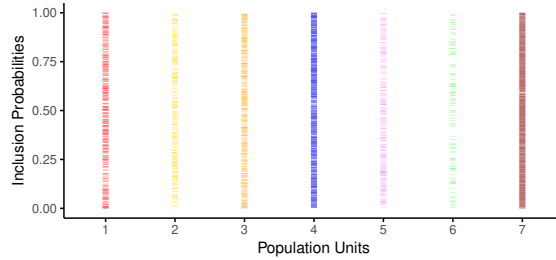


FIG 5. *Implementing of Algorithm 4 on the data of population (5) with $\alpha = .5$ and $M = 10,000$.*

The implementation of maximum entropy sampling through geometric approaches presents an intriguing alternative to complex mathematical algorithms. Maximum entropy design, as the holy grail of survey statistics, was first explored by Stern and Cover (1989) in lottery applications. While earlier foundational work was conducted by Hájek (1964, 1981), Hájek did not provide a concrete implementation methodology. Various implementation strategies have been proposed, including the draw-by-draw method, rejection sampling, and sequential algorithms (see Tillé, 2006). Chen and Liu (1997) catalogues diverse applications of maximum entropy design. Traditional implementation relies on Newton’s method for parameter calculation, which is computationally complex and prone to implementation errors. For example, while the `UPmaxentropy` function in the R package `sampling` (Tillé and Matei, 2015) enables maximum entropy design implementation, it exhibits limitations with large-scale problems. For instance, when working with a population size of 1000 and sample size $n = 450$, computational errors emerge¹.

On the other hand, maximum entropy sampling using the GFS approach offers several advantages. It demonstrates robust performance without computational errors, provides enhanced flexibility in achieving maximum entropy designs, and possesses the capability to incorporate additional constraints. This flexibility is particularly valuable when specific sampling conditions must be satisfied alongside maximum entropy objectives. Such conditions might include mandatory co-selection of certain sampling units, mutual exclusivity requirements between specific units, and balance constraints across various stratification variables. The GFS method’s adaptability allows researchers to tailor their sampling strategies to meet complex, multi-faceted requirements while still maintaining the desirable properties of maximum entropy designs.

While the maximum entropy using GFS approach offers numerous advantages, it’s worth noting that the method requires multiple iterations to effectively segment and distribute the FIP. This iterative process is necessary to achieve the desired spread and ensure maximum entropy. However, in the context of modern computing capabilities, including high-performance systems and the advent of quantum computing, the time required for these iterations becomes increasingly negligible. Even for very large populations, the computational demands of GFS are well within the scope of current technologies. As such, this characteristic of the method

¹For example, using `inclusionprobabilities(runif(N=1000), n=450)` generates the error: “missing value where TRUE/FALSE is required” in the condition `while (arr > eps)`.

poses no significant drawback in practical applications, allowing researchers to harness the full potential of maximum entropy sampling through GFS without concerns about computational limitations. By the way, it is possible to employ intelligent algorithms, such as genetic algorithms, to efficiently distribute the FIP and achieve maximum entropy designs more quickly.

5. Optimal GFS (OGFS)

As noted by Thompson and Seber (1996), there is no global optimal sampling design for finite population sampling. The optimality of a design depends on several factors, including the structure of the main variable, the FIP, and the estimator used. In discussing optimal design, the focus is on how, given a vector of FIP, it is possible to implement an unequal probability sampling method that outperforms conventional well-known sampling designs. It is also worth noting that, here this discussion primarily aims to enhance the design stage using the NHT estimator. Further research could explore improving both the design and estimation stages using GFS, which presents an interesting avenue for future investigation.

With OGFS, I illustrate how the GFS's ability to generate diverse designs opens a novel pathway, potentially offering a simple and efficient means for discovering new, effective designs.

In chaotic (random- or fixed-size) GFS, FIP remain fixed, facilitating the creation of designs with all possible SIP by rearranging the bars. Leveraging proper auxiliary variables, it becomes feasible to construct numerous designs. Once the position of bars (segments) are fixed, the design becomes fully known in GFS, enabling the calculation of criterion such as variance, maximum error, etc., of the NHT estimator based on some auxiliary variables. Therefore, one approach to searching for the optimal design involves, considering some criterion, rearranging the bars, changing SIP, creating different designs, and selecting the best one based on the criterion. As the most basic situation, consider two auxiliary variables x and z with some reasonable correlations with y , one for building FIP and another for evaluating designs based on some criterion. Using

$$\pi_k = \min(cx_k, 1), \quad \text{where} \quad \sum_{k \in U} \pi_k = n, \quad (8)$$

leads to FIP based on x with sample size n , known as PPS. In this design, we know that $\text{var}(\hat{X}) = 0$. Then using an evaluation variable z , consider a parameter, say θ_z , rearranging the bars a large number of times based on a random or intelligent algorithm, and selecting the best

arrangement to estimate θ_z based on the NHT estimator of z , results in selecting an optimal design.

Each searching design requires a criterion to assess its proximity to the desired outcome. In the context of optimizing GFS, various design parameters can be considered as criterion. The following equations outline three such criterion for OGPS:

$$\begin{aligned} C_1(\theta_z = Z, \mathbf{p}) &= \sum_{t=1}^T (\hat{Z}_{s_t} - Z)^2 p_t, \\ C_2(\theta_z = Z, \mathbf{p}) &= \sum_{t=1}^T |\hat{Z}_{s_t} - Z| p_t, \\ C_3(\theta_z = Z, \mathbf{p}) &= \max_{t=1, \dots, T} |\hat{Z}_{s_t} - Z|, \end{aligned}$$

where

$$Z = \sum_{k=1}^N z_k, \quad \hat{Z}_{s_t} = \sum_{k \in S} \frac{z_k}{\pi_k}.$$

An Intelligent Design Search Algorithm

A variation of a greedy best-first search approach is presented in this subsection to explore an optimal design. It begins with the initialization of auxiliary variables: x for constructing FIP and z for evaluating designs. An initial design is then established based on FIP, serving as the starting point for the optimization process.

The algorithm proceeds through several iterations, say Λ , where in each cycle, N_{node} number of new candidate designs are generated by modifying the last design based on Algorithm 4. This modification ensures the exploration of diverse configurations. Each new generated design undergoes evaluation based on predefined criterion, denoted as $C(\theta_z = Z, \mathbf{p})$. At the beginning, the initial design is considered the best design. Whenever a superior design is identified, it replaces the previous best design.

Two critical sets are set up during this process: the open set and the closed set. The open set maintains designs that are yet to be explored, prioritizing them based on their associated costs. In contrast, the closed set keeps track of designs that have already been evaluated, ensuring that the algorithm does not redundantly process the same design multiple times. Throughout the iterations, the algorithm tracks the most effective design. Then the set of potential designs

is managed to retain only the most promising candidates, replacing less efficient designs when necessary. This management ensures a focus on the most viable options for further refinement.

After all iterations are completed, the algorithm outputs the best design discovered, representing the optimal configuration according to the defined criterion. For further details, refer to Algorithm 5.

Algorithm 5 OGFS, A Greedy Best-First Search Version

```

1: Consider  $x$  as an auxiliary variable to construct, FIP,
2: Consider  $z$  as an evaluation variable and criterion  $C(\theta_z = Z, \mathbf{p})$  to evaluate designs,
3: Create the initial design based on the FIP and Algorithm 3,  $initial\_design$ ,
4: Initialize empty sets:  $open\_set \leftarrow \{\}$  (designs under exploration) and  $closed\_set \leftarrow \{\}$  (for explored designs),
5: Calculate the criterion for the  $initial\_design$ ,  $criterion$ ,
6: Add  $(criterion, initial\_design)$  to  $open\_set$ ,
7:  $best\_design \leftarrow initial\_design$ ,
8: for  $iterations = 1$  to  $\Lambda$  do
9:   Get the design with minimum  $criterion$  from  $open\_set$  and set it as  $current\_design$ ,
10:  for  $i = 1$  to  $N_{node}$  do
11:    Generate a  $new\_design$  by applying Algorithm 4 on  $current\_design$ ,  $new\_design$ ,
12:    Evaluate  $criterion$ ,  $C(\theta_z = Z, \mathbf{p})$  for  $new\_design$ ,  $new\_criterion$ ,
13:    if  $new\_design \notin closed\_set$  then
14:      if  $new\_criterion$  is better than  $criterion$  of  $best\_design$  then
15:        Update  $best\_design \leftarrow new\_design$ ,
16:      end if
17:      if size of  $open\_set < max\_open\_set\_size$  then
18:        Add  $new\_design$  to  $open\_set$ ,
19:      else
20:        Replace the design with maximum  $criterion$  in  $open\_set$  with  $new\_design$ ,
21:      end if
22:    end if
23:  end for
24:  Add  $current\_design$  to  $closed\_set$ ,
25: end for
26: return  $best\_design$ .

```

6. Simulations

To evaluate Algorithm 5 in finding optimal designs, we used the MU284 dataset from Särendal et al. (1992), which comprises data from 284 Swedish municipalities. To improve the clarity of our visualizations, we removed three outliers. These outliers were not leverage points and did not materially affect the results, as correlations remained consistent before and after their exclusion. This dataset includes variables with varying degrees of correlation to showcase a broad spectrum of relationships. The key variables used in the analysis are:

- y = P85: the 1985 population,
- x = P75: the 1975 population,
- x = S82: the total number of municipal council seats in 1982,

- $x = \text{REG}$: geographic region indicator,
- $z = \text{ME84}$: municipal employees in 1984,
- $z = \text{REV84}$: real estate values from the 1984 assessment,

The distribution and correlation of these variables are displayed in Figure 6. Here, P85 was used as the response variable y . For the design variable x and in constructing the FIP, four cases were considered: P75, which has the highest positive correlation with y in the dataset; S82, which shows a moderate positive correlation; REG, displaying a slight negative correlation; and finally, an equal probability sampling scenario. Additionally, for the evaluation variable z , ME84, a highly correlated variable with y , and REV84, another variable with substantial correlation, were used. To assess the role of OGPS, the following procedure was implemented:

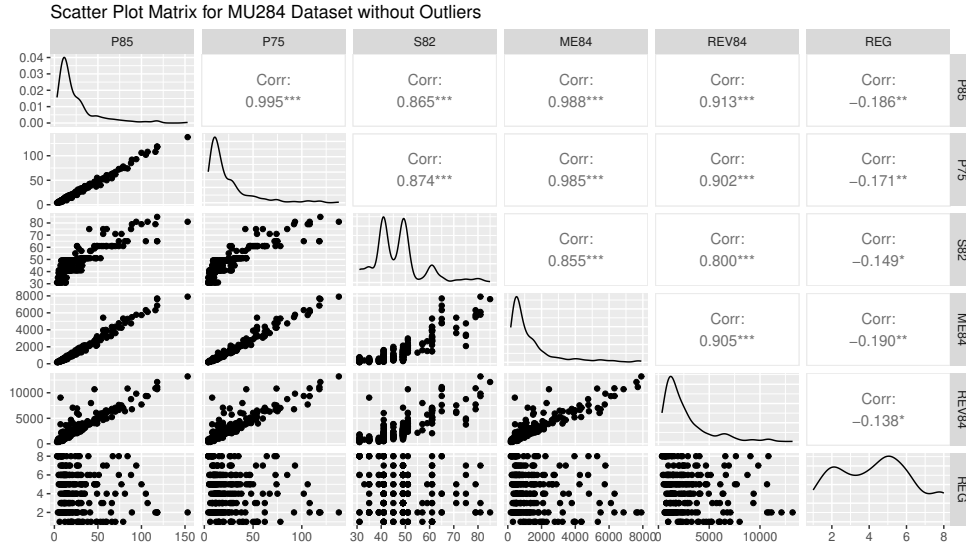


FIG 6. Distributions, scatter plots and significant linear relationships between six variables in the MU284 dataset after removing three outliers. Significance levels are indicated by symbols: * for p -value < 0.05 , ** for p -value < 0.01 , and *** for p -value < 0.001 .

1. First, FIP was constructed using x ,
2. For criterion,

$$C(\theta_z = Z, \mathbf{p}) = \sum_{t=1}^T (\hat{Z}_{s_t} - Z)^2 p_t,$$

has been used. Then, based on FIP and using z , the variance of the NHT estimator was calculated for five sampling designs, using the R package `sampling` Tillé and Matei (2015):

- MAX: Maximum Entropy Sampling,

- TIL: Tillé Sampling,
- MID: Midzuno Sampling,
- MAD: Madow Systematic Sampling,
- SRS: Simple Random Sampling without Replacement.

Please note that the variance (not its estimator) was calculated using SIP available for each design in the `sampling` package.

3. The GFS improvement was assessed using the following efficiency measures:

$$EF(y) = \frac{\text{var}(\hat{Y}_{\cdot})}{\text{var}(\hat{Y}_{\text{OGFS}})}, \quad EF(z) = \frac{\text{var}(\hat{Z}_{\cdot})}{\text{var}(\hat{Z}_{\text{OGFS}})}$$

where “.” indicates the best design among conventional designs MAX, TIL, MID, MAD, and SRS, and “OGFS” represents the OGFS design. It is notable that the optimal design among the conventional designs depended on the structure of the data and the type of FIP used for sampling.

For this simulation, specialized Python package is utilized, `geometric-sampling` (Panahbehagh et al. 2024), which implements the Geometric Sampling Method. This package served as the core framework for our simulations in this section, enabling efficient and accurate implementation of the sampling techniques discussed.

Results are presented in Table 1. The correlation of auxiliary variables x and evaluation variables z , denoted by $\rho_{x,y}$ and $\rho_{z,y}$ respectively. The parameters of Algorithm 5 were set as $\Lambda = 500$, $N_{node} = 5, 10, 20, 40$, $n = 14 (\simeq 0.05 \times N)$ and $\alpha = 1$. The initial efficiency measures, $EF_0(z)$ and $EF_0(y)$, indicate how the GFS performed at the outset compared to the best conventional design discussed earlier at the beginning of Section 6. Results can be summarized as follows based on the relationship between x and y :

- **High Positive Correlation:** Notably, the NHT estimator, when using FIP proportional to y , represents a highly efficient design. In an idealized scenario where this proportionality is perfect (though not achievable in practical situations), the variance of the NHT estimator would approach zero. For the case where $x = P75$, which has a correlation of 0.995 with y , the NHT estimator was indeed highly efficient. This made it challenging to optimize GFS to find a design that outperforms other standard PPS designs in terms of efficiency.

As shown in Table 1, when $z = \text{REV84}$ with a correlation of $\rho_{z,y} = 0.913$, no improvement was observed. However, when $z = \text{ME84}$, which has a higher correlation with y ($\rho_{z,y} = 0.988$), the GFS approach demonstrated moderate success. Given the strong relationship between x and y , this achievement is noteworthy.

- **Moderate Positive Correlation:** The case with $x = \text{S82}$ showed significant improvements in both $z = \text{REV84, ME84}$ and y . Based on its correlation with y , z contributed to an enhanced design for y , especially with a sufficiently large N_{node} .
- **Small Negative Correlation:** For $x = \text{REG}$, despite the weak negative correlation with y , both z and y showed notable improvements, particularly when N_{node} was increased. In this scenario, PPS designs were very inefficient, with SRS being more efficient than all PPS designs. Interestingly, however, even when the FIP are not proportional to y , the OGFS method is able to rearrange the bars and alter SIP in a way that results in an unequal probability design that surpasses the efficiency of SRS and, consequently, all other PPS designs. In this case, efficiency for y started with $\text{EF0}(y) = 0.29$ and rose to $\text{EF}(y) = 2.03$ across 500 iterations.
- **Equal Probability Sampling:** With $x = \text{Equal}$, z and y demonstrated considerable improvements in design quality, reflecting the effectiveness of OGFS.

In each of these scenarios, increasing the number of iterations led to a noticeable improvement in design quality. For example, considering $\Lambda = 5000$, and $N_{\text{node}} = 40$, the $\text{EF}(y)$, with $x = \text{REG}$ and $z = \text{REV84}$ increased significantly from 1.36 to 4.02.

While there are many parameters and options that can be investigated on Algorithm 5 and OGFS, for example α , n , Λ , etc, my aim here is not an exhaustive examination of the multifaceted advantages arising from innovations in GFS. Rather, the focus is on illustrating that applications employing innovative GFS methodologies yield diverse advantages and efficiencies. A comprehensive exploration of the outcomes of these innovations could serve as a viable subject for forthcoming independent articles.

It is crucial to highlight that the process of selecting the optimal design differs from simply testing multiple samples and choosing the best among them. Here, I construct numerous designs based on predetermined FIP, select the best among them, and then utilize this optimal design to select a sample. This method ensures an unbiased estimate. Conversely, assessing multiple samples and selecting the most accurate estimation, possibly utilizing auxiliary variables, can

TABLE 1

Efficiency of OGFS based on Algorithm 5 on data *MU284* using some auxiliary variables x , and evaluation variables z , with different correlation with the main variable y , denoted by $\rho_{\cdot,y}$ based on $\Lambda = 500$ iterations. $EF0(z)$ and $EF0(y)$ indicate the efficiency of GFS at beginning relative to the best conventional design introduced in Section 6.

$y = P85$		$N = 281$	$n = 14$				
z	x	N_{node}	$EF0(z)$	$EF(z)$	$EF0(y)$	$EF(y)$	
$\rho_{z,y} = .988$	ME84	P75	5	0.65	2.62	1.00	1.09
			10		5.77		1.08
			20		12.25		1.10
			40		44.34		1.07
$\rho_{x,y} = .995$	S82		5	0.95	1.70	0.96	1.70
			10		2.91		2.71
			20		4.55		4.13
			40		10.38		8.11
$\rho_{x,y} = -.186$	REG		5	0.29	0.61	0.29	0.63
			10		0.83		0.84
			20		1.21		1.21
			40		1.87		2.03
$\rho_{x,y} = 0$	Equal		5	1.00	5.37	1.00	4.91
			10		14.23		9.58
			20		46.90		20.58
			40		130.48		23.20
z	x	N_{node}	$EF0(z)$	$EF(z)$	$EF0(y)$	$EF(y)$	
$\rho_{z,y} = .913$	REV84	P75	5	1.00	1.90	1.00	0.92
			10		2.35		0.84
			20		3.25		0.75
			40		4.00		0.64
$\rho_{x,y} = .865$	S82		5	1.00	1.89	1.00	1.52
			10		3.69		1.92
			20		5.15		2.19
			40		11.29		2.51
$\rho_{x,y} = -.186$	REG		5	0.29	0.65	0.29	0.57
			10		0.93		0.79
			20		1.41		1.17
			40		1.99		1.36
$\rho_{x,y} = 0$	Equal		5	1.00	5.75	1.00	2.64
			10		13.71		3.12
			20		64.36		3.48
			40		188.61		3.42

lead to biased estimates.

7. Summary and Suggestions

A geometric sampling, GFS, has been introduced. GFS represents a new gate to the world of finite population sampling, offering a fresh perspective on sampling methodologies. This innovative approach appears to be essential in reshaping our understanding of sampling, thereby fostering increased creativity among researchers to devise new and efficient designs. With GFS, the simple act of rearranging segments allows for the creation and exploration of a diverse array of sampling designs, spanning from Madow designs (Madow 1949) characterized by relatively

low entropy to conditional Poisson sampling, known as maximum entropy sampling designs. Such depth of exploration was previously unattainable through conventional approaches reliant on mathematical algorithms.

It can be easily shown that other sampling designs such as simple random sampling, stratified sampling, systematic sampling, and most notably, multi-stage sampling, can be implemented using GFS by properly arranging the bars.

Chaotic GFS and OGPS represent two intriguing facets of the method. These can be applied to conventional designs to either increase their entropy or select an optimal design within them.

Beyond the greedy best-first search algorithm demonstrated in this study, this geometric framework opens doors to a wide array of intelligent algorithms in finite population sampling. For example, Genetic algorithms could be applied by treating segments as genes and their configurations as chromosomes, while other optimization techniques could be adapted to enhance sampling efficiency. This versatility marks a significant advancement in sampling methodology, promising innovative solutions to complex sampling challenges across various research domains.

For future research, it is intriguing to apply more intelligent algorithms, such as Genetic algorithms, A*, and others like simulated annealing or particle swarm optimization, for searching designs with maximum entropy, maximum efficiency, or even maximum spread (in data with coordinates) using GFS. The ability to arrange the bars arbitrarily, yet respecting the given FIP vector, makes GFS a powerful tool to innovate diverse and useful number of designs.

Acknowledgments

The author expresses sincere gratitude to three of his exceptionally talented students: Mehdi H. Moghadam, Mehdi Mohebbi, and AmirMohammad HosseiniNasab, for their invaluable contributions and insightful comments, particularly during the programming stage of this research.

References

- [1] Brewer, K. R. W. and Hanif, M. (1983). *Sampling with Unequal Probabilities*. New York: Springer.
- [2] Chen, X.-H. and Liu, J. S. (1997). Statistical applications of the Poisson-binomial and conditional Bernoulli distributions. *Statistica Sinica*, **7**, 875–892.

- [3] Hájek, J. (1964). Asymptotic theory of rejective sampling with varying probabilities from a finite population. *Annals of Mathematical Statistics*, **35**, 1491–1523.
- [4] Hájek, J. (1981). *Sampling from a Finite Population*. New York: Marcel Dekker.
- [5] Hansen, M. H. and Hurwitz, W. N. (1943). On the theory of sampling from finite populations. *Annals of Mathematical Statistics*, **14**, 333–362.
- [6] Horvitz, D. G. and Thompson, D. J. (1952). A generalization of sampling without replacement from a finite universe. *Journal of the American Statistical Association*, **47**, 663–685.
- [7] Jaynes, E. T. (1957). Information theory and statistical mechanics. *Physical Review*, **106**, 620.
- [8] Madow, W. G. (1949). On the theory of systematic sampling, II. *Annals of Mathematical Statistics*, **20**, 333–354.
- [9] Narain, R. D. (1951). On sampling without replacement with varying probabilities. *Journal of the Indian Society of Agricultural Statistics*, **3**, 169–174.
- [10] Panahbehagh, B., Mohebbi, M., HosseiniNasab, A., and Moghadam, M. H. (2024). geometric-sampling. <https://pypi.org/project/geometric-sampling/>.
- [11] Särndal, C.-E., Swensson, B., and Wretman, J. H. (1992). *Model Assisted Survey Sampling*. New York: Springer.
- [12] Stern, H. and Cover, T. M. (1989). Maximum Entropy and the Lottery. *Journal of the American Statistical Association*, **84**, 980–985.
- [13] Thompson, S. K. and Seber, G. A. F. (1996). *Adaptive Sampling*. Vol. 231 of Wiley Series in Probability and Statistics. New York: Wiley. Hardcover edition. ISBN: 978-0471965277.
- [14] Tillé, Y. (2006). *Sampling Algorithms*. New York: Springer.
- [15] Tillé, Y. (2020). *Sampling and Estimation From Finite Populations*. Hoboken: Wiley.
- [16] Tillé, Y. and Matei, A. (2015). sampling: Survey Sampling. *R package version 2.7*.